2018 European Control Conference (ECC)
June 12-15, 2018. Limassol, Cyprus

Robust dynamic allocation for aircraft roll-out phase directional control

M. Cassaro[1], C. Roos[1] and J-M. Biannic[1]

Abstract— **This paper addresses the robust allocation problem for the directional control of on-ground aircraft. Motivations rely on the need of extending automatic control capabilities across the entire roll-out phase, allocating accordingly to diverse constraints. The objective is to design an original control architecture, able to inherently compensate for changes in the plant's state and control matrices, while guaranteeing robustness towards disturbances and performances demanded by civil aviation regulation. Main contributions consist of synthesizing an H_∞ optimized guidance control loop based on differential braking force, together with implementing an original modification of an available control allocation methodology to properly include rudder and nose wheel steering actions. Control design techniques are detailed and simulation results illustrate the validity and efficacy of the proposed control architecture.**

I. INTRODUCTION

Most airborne phases of commercial flights have been automated with the development of fly-by-wire solutions. However, after touchdown, the motion of the aircraft is still manually controlled by the pilot using thrust, rudder deflection, nose wheel steering and brakes. This is especially demanding in adverse conditions such as wet runway and severe crosswind. So it is not surprising that most accidents over the last 20 years have occurred during landing, with runway excursions representing the biggest cause of hull losses by accident [1]. Following a study carried out by the International Civil Aviation Organization (ICAO), the count of runway excursions has not decreased over the last 20 years [2]. Factors leading to runway excursions analyzed in [3] are mainly due to wet/contaminated runways, crosswind and nose wheel steering problems.

Thus, there is a real need to design autopilots for ground phases. The control objectives depend on the aircraft velocity. At low speed, the main concern is maneuverability. Between 40 and 80 kts, the main issue is to deal with the varying effectiveness of the control devices: the nose wheel becomes less efficient as speed increases, and conversely for the rudder due to larger aerodynamic effects. Finally above 80 kts, the objective is to ensure the safety of operations.

Existing directional control approaches mostly relies on nose-wheel steering system only, see *e.g.* [4], [5], [6], [7]. Moreover, when treated as a control allocation problem, see *e.g.* [8], [9], [10], [11], differential braking is systematically ignored.

One of the very few works facing a similar control allocation problem is [12]. However, it presents a very simple allocation solution depending on the aircraft velocity V_x: only the nose wheel or the rudder is used if $V_x < V_{low}$ or $V_x > V_{high}$, and in between a linear blend is applied. This kind of approach is typically implemented by aircraft manufacturers due to its simplicity, but it is clearly suboptimal. A less naive approach would, however, allow to improve on-ground performances during worst-case scenarios such as landing on contaminated runway with severe crosswind.

As already mentioned above, one of the most challenging on-ground control problems occurs at intermediate speed between 40 and 80 kts. The main objective is tracking the runway centerline in worst-case scenario conditions. Guaranteeing robustness and achieving good performances inevitably requires the combination of all available actuators, and notably to use differential braking in conjunction with classical control devices.

The main contribution of the present work is to address the aforementioned control problem, which is still an open issue to the best of our knowledge. Using an accurate yet tractable on-ground aircraft model developed in a companion paper [13], a dynamic control allocation scheme is implemented based on the method of [9], so as to account for the abrupt changes in the actuators effectiveness due to the fast variations of aircraft velocity and loads during the roll-out phase. A robust outer loop designed using structured H_∞ tools allows to cope with severe crosswind and to limit the aircraft lateral deviation, even on a wet or snowy runway.

The paper is organized as follows. The considered on-ground aircraft model is briefly described in Section II. The control problem is then presented and solved in Section III. Detailed numerical results are finally reported in Section IV.

II. AIRCRAFT ON-GROUND LPV MODEL

The considered on-ground aircraft model is briefly described in this section. Only the main equations and assumptions are highlighted, but more details and justifications can be found in the companion paper [13]. The model is valid on the main runway, during both take-off and landing for longitudinal velocity $V_x \in [40;\ 100]$ knots, and with small crosswind in the $\vec{x_b}\vec{y_b}$ plane (up to 5 knots), see Fig. 1. The following assumptions are made in order to simplify the general nonlinear equations, yielding a model of tractable complexity adapted for control design:

(A1) Tricycle hypothesis.
(A2) Linearized expressions for the aerodynamic effects.
(A3) Rigid aircraft and shock absorbers, and planar motion (no pitch rate, roll rate and vertical velocity), yielding same load on left and right main landing gears.
(A4) Symmetrical engines thrust T_{eng} aligned with the fuselage reference axis $\vec{x_b}$.

[1] Information Processing and Systems Department, ONERA - The French Aerospace Lab, Toulouse, France, mario.cassaro@onera.fr

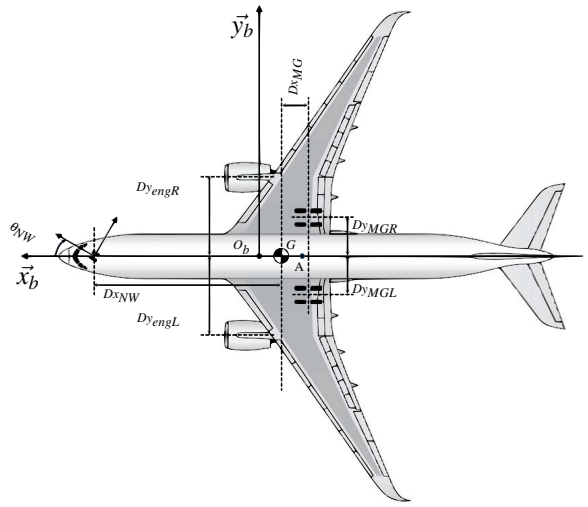

Fig. 1. Body reference system $\mathscr{R}_b$

(A5) Small angles approximation, including the nose wheel steering angle θ_{NW}.
(A6) Velocity of main landing gears wheels center equal to that of the aircraft center of gravity G.

Thanks to assumptions *(A1,A2,A3)*, the equations of motion in the body reference system $\mathscr{R}_b$ are obtained:

$$\begin{array}{rcl} \dot{V}_x & = & F_x/m + rV_y \\ \dot{V}_y & = & F_y/m - rV_x \\ \dot{r} & = & M_r/I_{zz} \end{array} \tag{1}$$

where V_y, r, m and I_{zz} are the lateral velocity, the yaw rate, the aircraft mass and the inertia around the $\vec{z_b}$ axis respectively. The aircraft yaw angle ψ is computed as $\dot{\psi} = r$.

The external forces and moment in equation (1) are of three different origins, precisely propulsive, aerodynamic and the ground reaction:

$$\begin{array}{rcl} F_x & = & T_{eng} + F_{xa} + F_{xg} \\ F_y & = & F_{ya} + F_{yg} \\ M_r & = & M_{ra} + M_{rg} \end{array} \tag{2}$$

T_{eng} only appears in F_x according to assumption *(A4)*. Linearized expressions of the aerodynamic effects F_{xa}, F_{ya} and M_{ra} are considered according to *(A2)*, accounting for rudder deflection δ_r as well as longitudinal and lateral wind components W_x and W_y. Details are omitted for the sake of brevity.

Ground reaction forces are of two natures: rolling resistance and slip force. The nose wheel is a free rolling wheel (*i.e.* neither driven nor braked) and therefore is subject only to rolling resistance F_{r_k} and lateral slip force F_{sy_k}. The main landing gears wheels are potentially braked, and the longitudinal slip force F_{sx_k} is to be considered in addition. These forces act along the $\vec{x_k}$ and $\vec{y_k}$ axes of the tires, where k refers to the nose wheel (NW) or the left (resp. right) main landing gear wheel (MGL (resp. MGR)). First, rolling resistance can be computed as:

$$F_{r_k} = \mu_r F_{z_k} \tag{3}$$

where $\mu_r = \bar{\mu}\mu_{rMAX}$ depends on the characteristics of the surface in contact with the wheels. The relative friction coefficient $\bar{\mu}$ depends on the runway state, and μ_{rMAX} denotes the maximum rolling friction coefficient for a dry runway. The normal reaction F_{zk} is function of V_x and can be computed at each landing gear by a moment balance around $\vec{y_b}$:

$$\begin{array}{rcl} F_{z_{NW}} & = & \dfrac{mgD_{xMG} - F_{za}\left(D_{xMG} + (x_A - x_G)\right)}{D_{xNW} + D_{xMG}} \\ F_{z_{MGR/L}} & = & \dfrac{mgD_{xNW} - F_{za}\left(D_{xNW} - (x_A - x_G)\right)}{2(D_{xNW} + D_{xMG})} \end{array} \tag{4}$$

x_G and x_A are the x-coordinates of G and of the point A where the aerodynamic effects are applied. D_{xNW} and D_{xMG} are positive distances shown in Fig.1, and g is the standard gravity. Following [14], the longitudinal and lateral slip forces are then modeled as:

$$F_{sx_k} = N_{t_k}\ \mathrm{sat}_{\left[\bar{\mu}\lambda_{sx_k}\frac{F_{z_k}}{N_{t_k}}\right]}\left(K_{x_k}T_{brk_k}\right) \tag{5}$$

$$F_{sy_k} = -N_{t_k}\ \mathrm{sat}_{\left[\bar{\mu}\lambda_{sy_k}\frac{F_{z_k}}{N_{t_k}}\right]}\left(K_{y_k}\beta_k\frac{F_{z_k}}{N_{t_k}}\right) \tag{6}$$

K_{x_k} and K_{y_k} correspond to the inverse of the effective rolling radius and the reduced lateral cornering gain respectively. K_{y_k} is not function of V_x in the operating domain, but it depends on the runway state as follows:

$$K_{y_k} = \frac{K_{yMAX_k}}{\frac{2}{3} + \frac{1}{3\bar{\mu}}} \tag{7}$$

where K_{yMAX_k} is the reduced lateral cornering gain for a dry runway. λ_{sx_k} and λ_{sy_k} denote the longitudinal and lateral friction fractions satisfying ${\lambda_{sx_k}}^2 + {\lambda_{sy_k}}^2 = {\mu_{MAX}}^2$, where μ_{MAX} is the tire-road friction coefficient for a dry runway. N_{t_k} is the number of tires, and T_{brk_k} represents the braking torque. The saturation operator is defined as $\mathrm{sat}_{[F]}(x) = x$ if $|x| < F$ and $\mathrm{sat}_{[F]}(x) = F$ otherwise. Under assumptions *(A1,A3,A5,A6)*, the sideslip angles β_k can be computed as:

$$\begin{array}{rcl} \beta_{NW} & = & \dfrac{V_y + rDx_{NG}}{V_x} - \theta_{NW} \\ \beta_{MGR} & = & \beta_{MGL} \underbrace{=}_{(A6)} \beta_G = \dfrac{V_y}{V_x} \end{array} \tag{8}$$

Finally, $\sin\theta_{NW}$ and $\cos\theta_{NW}$ can be replaced with θ_{NW} and 1 respectively thanks to assumption *(A5)*. So the total contact forces and moments in $\mathscr{R}_b$ are given by:

$$\begin{array}{rcl} F_{xg} & = & -F_{r_{NW}} - F_{r_{MGR}} - F_{r_{MGL}} - F_{sy_{NW}}\theta_{NW} - F_{sx_{MGR}} - F_{sx_{MGL}} \\ F_{yg} & = & -F_{r_{NW}}\theta_{NW} + F_{sy_{NW}} + F_{sy_{MGR}} + F_{sy_{MGL}} \\ M_{rg} & = & \left(F_{sy_{NW}} - F_{r_{NW}}\theta_{NW}\right)D_{xNW} - \left(F_{sy_{MGR}} + F_{sy_{MGL}}\right)D_{xMG} \\ & & + \left(F_{sx_{MGR}} + F_{r_{MGR}}\right)D_{yMG} - \left(F_{sx_{MGL}} - F_{r_{MGL}}\right)D_{yMG} \end{array} \tag{9}$$

The rudder and the nose-wheel steering system are modeled as first-order systems with magnitude and rate saturations. The braking system dynamics is neglected since it is much faster than the aircraft one. Therefore, it is assumed that commanded braking forces $F_{brk_k} = T_{brk_k}/D_{y_k}$ directly apply to the main landing gears. Moreover, the control input for differential braking is $\delta_{BR} = \left|F_{brk_{MGR}}\right| - \left|F_{brk_{MGL}}\right|$, whose sign respects the convention on the yaw moment [17]. The thrust T_{eng} exerted by the engines is kept constant to idle

value during roll-out phase and, so forth, is not considered in the sequel. Finally, the sensors dynamics is neglected because much faster than the aircraft one. To sum up, the considered model has 3 control inputs ($\delta_{r_c}, \theta_{NW_c}, \delta_{BR}$), 2 external disturbances (W_x, W_y), 8 states (V_x, V_y, r, ψ and 4 actuators states), and 7 measured outputs ($V_x, V_y, r, \dot{r}, \theta_{NW}$ and the longitudinal and lateral load factors $N_x = \dot{V}_x/g, N_y = \dot{V}_y/g$).

Validation against an in-house high-fidelity Airbus simulator demonstrates a very good level of accuracy [13], which coupled to its reasonable complexity, makes the proposed model tractable for control laws design.

III. PROBLEM FORMULATION

The directional control of an aircraft on-ground during roll-out phase is a 2D trajectory tracking problem of an over-actuated nonlinear system subject to external disturbances. The control objective is to track the runway centerline compensating for plant state and control matrices time varying parameters, guaranteeing robustness against gusts and tracking performances in the entire domain of operation. The proposed approach consists of treating separately the guidance and the dynamic allocation problems. This allows the robustness and performance constraints to be addressed independently of the stability of the allocated closed loop. To this purpose, the general architecture chosen for control synthesis is depicted in Fig. 2 and consists of a guidance outer loop in cascade with an additive dynamic allocator. The guidance law objective is to compensate the lateral deviation error $y_e = y_{ref} - y_{act}$, defined as the difference between reference and actual lateral positions. A reduced set of the observable states is assumed to be available for feedback, namely $x_{obs} = [y \quad V_y \quad \psi \quad r]^T_{act}$. A single control command is output by the guidance law and allocated afterwards. Noting that the allocator dynamics does not affect the response of the plant, the chosen control signal is necessarily the differential braking force $y_c = \delta_{BR}$. Among the three available control actions, it is indeed the only one effective across the entire roll-out speed range and so able to meet performance and robustness requirements. The guidance law output $\bar{y}_c = [0 \quad \delta_{BR} \quad 0]^T$ is completed by zeros to permit allocation to the full set of available control commands $u = [\delta_r \quad \delta_{BR} \quad \delta_s]^T$, where $\delta_r = \delta_{r_c}$ and $\delta_s = \theta_{NW_c}$ for the rest of the paper. This architecture allows for pursuing the most appropriate allocation strategy, without jeopardizing the level of performance achieved by the outer loop.

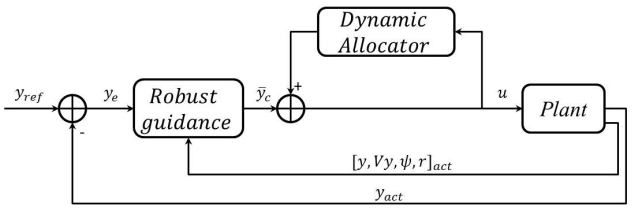

Fig. 2. Control architecture with dynamic control allocator in cascade

A. H_∞ synthesis for robust guidance

Structured H_∞ synthesis is used in this application for robust guidance law design [16]. The optimization process is carried out by means of the *systune* routine implemented in the *Robust Control* toolbox for Matlab. The model is linearized around a certain speed value and re-casted in a standard LTI state space formulation, with states x and controls u defined as above. The signals feeding the controller are the four measured states, in addition to the lateral deviation error y_e and its integral. The controller output is the single δ_{BR} command. The optimization of the static gains vector $G_{H_{\infty_{6\times1}}}$ is performed by considering the lateral gust as an exogenous disturbance on the control input u and minimizing sensitivity with respect to tracking error and control energy. The correctness of this assumption relies on the fact that lateral gusts act on the aircraft by generating a sideslip angle and consequently a yaw moment [17], which is the same effect as the control command taken into account. Considering a standard formulation for H_∞ optimization [15], [18], a dynamic weight on the tracking error and a static gain on the control input are introduced, respectively $W_{tr}(s) = 100\,(1/s + 0.001)$ and $W_u = 0.1$. The tracking error is evaluated with respect to a second order reference model with suitable characteristics chosen to be admissible to the aircraft on-ground dynamics, *i.e.* $\zeta = 0.7$ and $\omega_n = 0.4$ rad/s. Once the desired trade-off between performances and disturbances rejection is achieved for the considered speed, the process is repeated for other speed values. Finally, the obtained vectors of gains are stacked in a matrix and interpolated in function of V_x to obtain a scheduled control strategy. Note that an LPV design method could have been chosen also, but this is not the central issue of the paper. The need of such procedure is justified by the LPV nature of the plant, which impedes a single step solution of the problem, if both performance and robustness constraints must be met.

B. Dynamic control allocation

The on-ground aircraft model considered in this paper belongs to a class of LPV plants which can be described as follows:

$$\begin{aligned} \dot{x}(t) &= A(p(t))x(t) + B(p(t))u(t) + B_d(p(t))d(t) \\ y(t) &= C(p(t))x(t) + D(p(t))u(t) + D_d(p(t))d(t) \end{aligned} \tag{10}$$

where $p(t) \in \mathscr{P} \subset \Re^{n_p}$ are the time-varying parameters, and $x(t) \in \Re^n$, $u(t) \in \Re^{n_u}$, $d(t) \in \Re^{n_d}$ and $y(t) \in \Re^{n_y}$ are respectively the plant state, input, disturbance and output vectors. The proposed dynamic allocator design for such a class of models is based on theory developed in [9] and extended by the authors to the LPV case. Recalling the input redundant assumption formalized in [9] and assuming that the dependency to the time-varying parameters does not affect the rank of the matrices, the following definition holds:

Definition 1: The plant (10) is *strongly input redundant* if $Ker\left(\begin{bmatrix} B(p(t)) \\ D(p(t)) \end{bmatrix}\right) \neq \varnothing$ for all $p(t) \in \mathscr{P}$. In this case, let the parameter-dependent matrix $B(p(t))_\perp$ be defined as:

$$Im(B(p(t))_\perp) = Ker\left(\begin{bmatrix} B(p(t)) \\ D(p(t)) \end{bmatrix}\right) \tag{11}$$

Under this condition, for a given stable non-allocated outer-loop controller with output $y_c \in \Re^{n_{y_c}}$ so that $n_{y_c} < n_u$, and defining $y_{c_{adj}} \in \Re^{n_{y_{c_{adj}}}}$ a zero vector of dimension $n_{y_{c_{adj}}} = n_u - n_{y_c}$, it is possible to design an inherently stable dynamic allocator of the form:

$$\begin{aligned} \dot{w}(t) &= -KB_{\perp}^{T}(p(t))\overline{W}u(t) \\ u(t) &= \overline{y_c}(t) + B_{\perp}(p(t))w(t) \end{aligned} \tag{12}$$

where $\overline{y_c} = [y_c \quad y_{c_{adj}}]^T$ and the two symmetric matrices K and $\overline{W}$ are weight matrices, whose properties are discussed in the following. The closed-loop stability of the time-invariant version of (12) is proven in [9]. In detail, under the hypotheses:

(H1) $K > 0$

(H2) $B_{\perp}^{T}\overline{W}B_{\perp} > 0$

the allocated control system is internally stable if and only if the non-allocated closed-loop system is internally stable. This is proven by observing that the plant output y is not affected by the allocator dynamics w since $BB_{\perp} = 0$ and by verifying that w has a converging dynamics since all the eigenvalues of its state matrix $-KB_{\perp}^{T}\overline{W}B_{\perp}$ are strictly negative thanks to assumptions *(H1)* and *(H2)*. Note that this result is guaranteed for any full rank matrix $B_{\perp}$ if $\overline{W}$ is chosen to be positive definite. So if the latter assumption is satisfied, considering a parameter varying $B_{\perp}(p(t))$ does not affect the validity of this proof and so forth, the stability of the system is guaranteed under the prescribed conditions.

To employ formulation (12), the aircraft model has to be reduced to satisfy the *strongly input redundant* hypothesis and allow $B_{\perp}$ computation. In this context, the plant observable states are reduced to the lateral velocity and the yaw rate, *i.e.* $x_{red} = [V_y \quad r]_{act}^{T}$, while the inputs $u = [\delta_r \quad \delta_{BR} \quad \delta_s]^T$ are the same as before. This leads to the following control matrix in compact form:

$$B_{red} = \begin{bmatrix} \frac{1}{2}\rho SV^2 C_{y_{\delta_r}}/m & \frac{1}{2}\rho SV^2 \bar{c} C_{n_{\delta_r}}/I_{zz} \\ 0 & G_{BR}D_{y_{MG}}/I_{zz} \\ G_s/m & G_s D_{x_{NG}}/I_{zz} \end{bmatrix}^T \tag{13}$$

G_s and G_{BR} are defined as cornering gains for steering and differential braking actions respectively. $C_{y_{\delta_r}}$ and $C_{n_{\delta_r}}$ are aerodynamic stability derivatives, and ρ, S, $\bar{c}$ are the air density, the reference surface and the mean aerodynamic chord length respectively. It is worth noticing that only the rudder components depend on velocity $V \approx V_x - W_x$ when design is concerned, whereas for validation purposes the allocator is applied to the full model described in Section II, with all the described dependencies. The choice of K and $\overline{W}$ affects respectively the transient behavior of the allocator and the final distribution of the control commands. High values of K cause faster responses with the risk of introducing instabilities, while high values of certain $\overline{W}$ components amount to penalizing the associated control actions. In the present contect, the objective is allocating in a prescribed way across a varying speed domain, so the $\overline{W}$ components are formulated as functions of the actual aircraft speed, *i.e.* $\overline{W}(V_x) = \mathrm{diag}(\overline{W}_{\delta_r}(V_x), \overline{W}_{\delta_{BR}}(V_x), \overline{W}_{\delta_s}(V_x))$.

IV. RESULTS AND DISCUSSION

The control architecture presented in this paper is analyzed in this section by simulation and results are discussed. The realistic test case scenario chosen for validation purpose is as follows: the guidance law robustness and performance are first evaluated in absence of control allocation; the dynamic control allocator properties described in Section III-B are then demonstrated; and finally, a predefined actuation strategy function of the aircraft speed is introduced and proven to be effective in the entire on-ground operating domain.

A. Test case scenario

A realistic test case scenario has been defined, in conjunction with industrial partners, to guarantee correctness, consistency and completeness for validation purpose of the proposed control architecture. It consists of a roll-out maneuver with inexact touch-down point, followed by a deceleration phase in presence of lateral gust and a final phase of taxiing with a change of line maneuver. In detail, initial conditions are: $|\Delta y| = 5m$ and $V_x = 80m/s$. Deceleration to $V_x = 10m/s$ is disturbed by a gust $W_y = 10m/s$, simulated by a persistent step starting at $50\,s$ of simulation. When reaching taxi speed of $V_x = 10m/s$, a change of line of $|\Delta y| = 25m$ is applied at $75\,s$ of simulation. The following requirements have to be respected during simulation:

Performance requirements

- Aircraft lateral excursion shall be limited to $y = 5m$ during roll-out deceleration
- Longitudinal load factor shall be limited to $N_x = 0.35$
- Actuator wear shall be minimized (using the most appropriate actuation system for each phase)

Robustness requirements

- Crosswind disturbance rejection
- Tolerance to state and control matrices time variations

B. Robust guidance law

The preliminary objective is to verify the robustness of the guidance law, designed as in Section III-A, since the dynamic allocator does not modify the plant outputs as it will be proven later on. First, the single control input (δ_{BR}) version of the aircraft on-ground model is linearized and used for structured H_∞ control optimization at three different speed values (10, 40 and $80m/s$). The obtained controller is made of a matrix $G_{H_{\infty_{6\times 3}}}$ of static gains fed by $y_e, \int y_e, y, V_y, \psi$ and r. It is interpolated, so that it can be used on the whole speed range. Then, robustness is verified in simulation on the complete LPV aircraft model against parametric uncertainties and external disturbances, while a maneuver is being performed to reach the runway center-line after an initial $5m$ lateral deviation. For the model parameters, a level of uncertainties of $\pm 10\%$ around the nominal value is considered for all the aerodynamic and wheels' cornering gain coefficients. A relevant number of simulations is run by randomly choosing the parameters within their bounded set. The external disturbance consists of an additive and persistent random lateral wind $W_{y_{rand}}$ of standard deviation

$5m/s$. Simulations are run by randomly selecting a value of the horizontal speed in the range $V_x = [10\ -\ 80]m/s$, and an additional lateral gust $W_{y_{step}}$ within $\pm 10m/s$, always applied at $10s$ of simulation.

Results reported in Fig. 3, where the optimized guidance control law is applied to the complete LPV aircraft on-ground model, demonstrate a very robust behavior of the non-allocated control system to the considered uncertainties and disturbances. As a matter of fact, the time response remains bounded and performance is satisfactory in the entire set of random combinations evaluated.

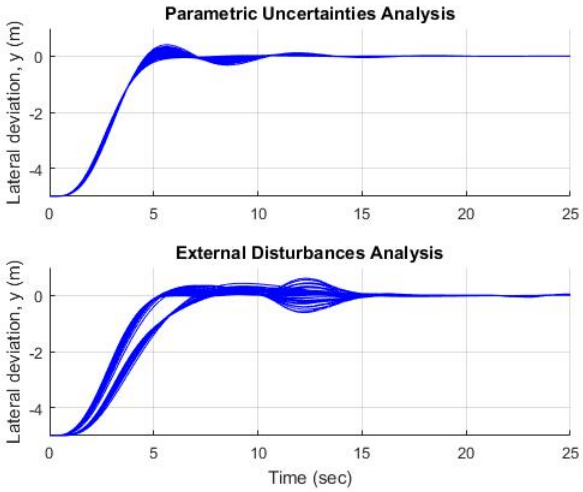

Fig. 3. Closed loop response: Robustness analysis against parametric uncertainties (top), and external disturbances (bottom)

C. Dynamic allocation

The properties of the proposed dynamic allocator are investigated in this section. To the purpose of demonstrating the invariance of the plant output to the allocator dynamics it is reported, in Fig. 4, the same maneuver performed with and without allocator. The test case scenario is similar to Fig. 3, but at a constant horizontal speed of $V_x = 80m/s$ and with a maximum gust of $W_{y_{step}} = -10m/s$ at $50s$. The exact correspondence of the plant response in terms of lateral deviation y can be clearly noticed. Simultaneously, the control commands differ noticeably when external gust is applied. The same effect is not noticeable at the beginning of the simulation because the maneuver is faster than the allocator dynamics. In this case the weight matrices are chosen to be $K = 0.1$ and $\overline{W} = I$ to demonstrate the pure effect of the allocation formulation and to justify the need of a predefined allocation strategy. In fact, always from Fig. 4, it can be seen how the allocator so designed redistributes the signal among all the three available actuation systems without any specific criteria.

Meeting the performance requirements on the actuation wearing practically means to be always able to allocate to the most efficient actuation system, avoiding unnecessary control overlapping. For the sake of clarity, recalling the proposed research motivation, it must be guaranteed that at

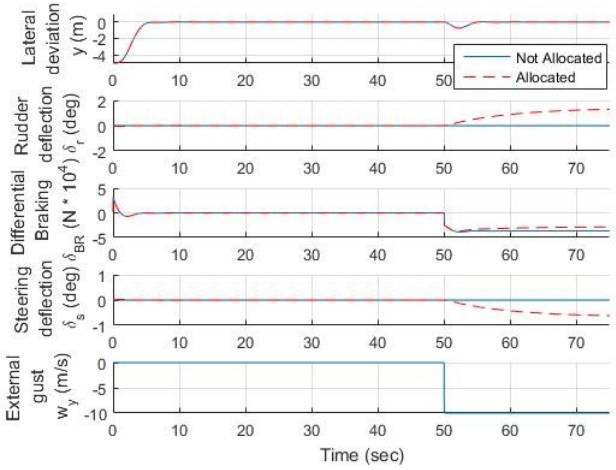

Fig. 4. Closed loop response: non allocated *v.s.* allocated without predefined strategy, $V_x = 80\ m/s$

high speed, $40 < V_x < 80\ m/s$, only the rudder is controlling directionally the aircraft because it is still effective and also because brakes are employed for decelerating the aircraft. On the other hand, at very low speed $0 < V_x < 10\ m/s$, only steering control is capable of governing the aircraft without extra actuation. Even if effective among the whole speed range, the differential braking control, which can be considered the main contribution of the present paper, has to be employed only when the other two actuation systems are not effective to avoid excessive wear, which means for $10 < V_x < 40m/s$. For smooth transition in allocating among the three available actuation systems, avoiding discontinuous behaviors, a variable weight matrix $\overline{W}(V_x)$ is implemented as in Fig. 5. The sigmoid and bell functions are detailed in the legend for numerical value information.

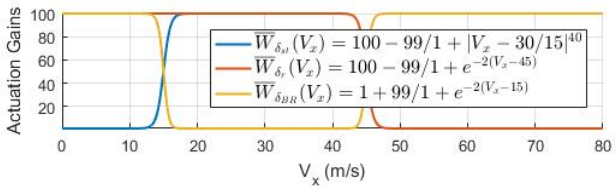

Fig. 5. Speed dependent allocation strategy

Finally, the complete control architecture, made of the allocator, with assigned variable gain strategy, in cascade with the scheduled robust guidance law is applied to the complete model and validated in the full test case scenario described in Section IV-A. Results are reported in Figs. 6 and 7, showing respectively the initial $75s$ of simulation for states and controls, and the response to a line change maneuver during taxi. From Fig. 6 the robustness of the response can be assessed when maneuvers and gust rejection are performed at varying speed. Jointly, the constraint on the longitudinal load factor is respected and control is accomplished with realistic values of the observed states. Analyzing the controls' time histories in Figs. 6 and 7, the effectiveness of the proposed solution is clearly demonstrated

by finding the control action mostly allocated to the rudder at the beginning of the simulation, to differential braking at middle speed range, when gust disturbance is acting, and to steering only at very low taxi speed for the line change maneuver.

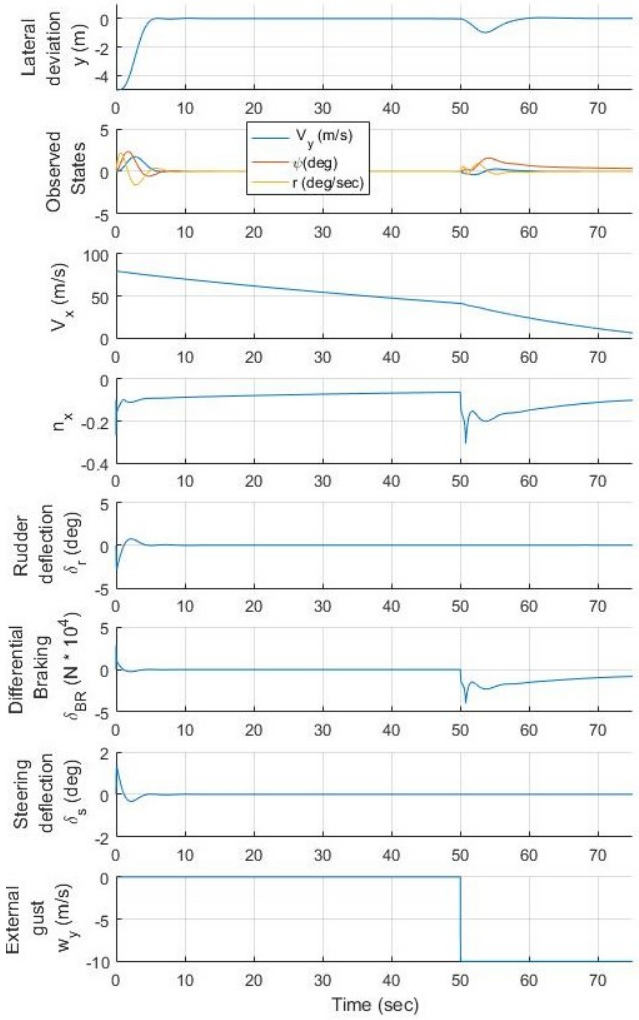

Fig. 6. Full test case scenario, states and control monitoring

V. CONCLUSIONS

An architecture has been presented in this paper to solve the robust dynamic allocation problem of aircraft on-ground directional control during roll-out phase. The formulation employed allows to decouple the robustness and performance requirements from the allocation tasks. An original guidance law, based on differential braking command, has first been optimized by structured H_∞ formulation, and results proving its efficacy have been reported. The dynamic allocation procedure has then been detailed, and its properties have been demonstrated and extensively discussed. The promising results of the proposed approach let the authors aim at experimental tests for further investigation and validation. The targeted benefit is easier and safer piloting in adverse environmental conditions and aircraft failure conditions.

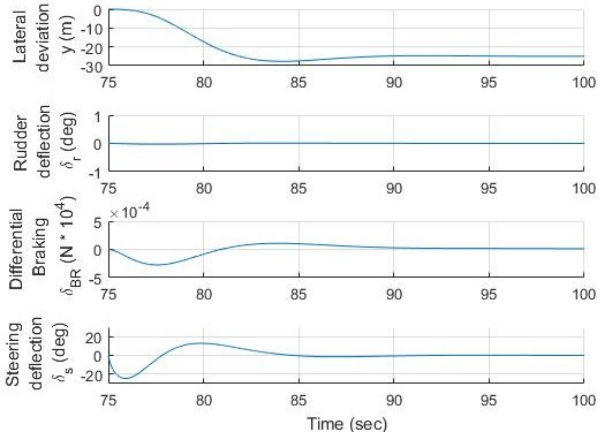

Fig. 7. Taxing phase, lateral deviation and controls

REFERENCES

[1] Airbus, A statistical analysis of commercial aviation accidents 1958-2016, Tech. Rep., January 2017.

[2] Eurocontrol, European action plan for the prevention of runway excursions - Edition 1.0, Tech. Rep., January 2013.

[3] G. van Es, A study of runway excursions from a european perspective, Eurocontrol, Tech. Rep. NLR-CR-2010-259, 2010.

[4] C. Roos, J-M. Biannic, S. Tarbouriech, C. Prieur and M. Jeanneau, On-ground aircraft control design using a parameter-varying anti-windup approach, Aerospace Science and Technology, 14(7):459–471, 2010.

[5] J. Duprez, F. Mora-Camino and F. Villaumé, Control of the aircraft-on-ground lateral motion during low speed roll and manoeuvers, in Proceedings of the IEEE Aerospace Conference, pages 2656–2666, Big Sky, MT, 2004.

[6] F. Re, Modelica landing gear modelling and on-ground trajectory tracking with sliding mode control, in Advances in Aerospace Guidance, Navigation and Control, pages 103–114, Springer, 2011.

[7] D. Lemay, Y. Chamaillard, M. Basset and J-P. Garcia, Gain-scheduled yaw control for aircraft ground taxiing, in Proceedings of the 18th IFAC World Congress, pages 12970-12975, Milano, Italy, 2011.

[8] T. Johansen and T. Fossen, Control allocation – A survey, Automatica, 49(5):1087–1103, 2013.

[9] L. Zaccarian, Dynamic allocation for input redundant control systems, Automatica, 45:1431–1438, 2009.

[10] O. Härkegård, Dynamic control allocation using constrained quadratic programming, Journal of Guidance, Control, and Dynamics, 27(6):1028–1034, 2004.

[11] Y. Luo, A. Serrani, S. Yurkovich, D. Doman, and M. Oppenheimer, Dynamic control allocation with asymptotic tracking of time-varying control trajectories, in Proceedings of the American Control Conference, pages 2098–2103, Portland, OR, 2005.

[12] G. Looye, Rapid prototyping using inversion-based control and object-oriented modeling, in Nonlinear Analysis and Synthesis Techniques for Aircraft Control, pages 147–173, LNCIS, Springer, 2007.

[13] E. Sadien, C. Roos, A. Birouche, C. Grimault, L-E. Romana, J. Boada-Bauxell and M. Basset, Design oriented modeling of an on-ground aircraft, in Proceedings of the European Control Conference, Limassol, Cyprus, 2018.

[14] J-M. Biannic, A. Marcos, M. Jeanneau and C. Roos, Nonlinear simplified LFT modeling of an aircraft on-ground, in Proceedings of the IEEE Conference on Control Applications, pages 2213–2218, Munich, Germany, 2006.

[15] K. Zhou, J. C. Doyle and K. Glover, Robust and Optimal Control, Prentice Hall, 1996.

[16] P. Apkarian and D. Noll, Nonsmooth H_∞ Synthesis, IEEE Transaction on automatic control, 51(1):71–86, 2006.

[17] B. Etkin and L. Reid, Dynamics of flight: stability and control, 3rd Edition, Wiley, 1995.

[18] J-M. Biannic and C. Roos, Flare control law design via multi-channel H_∞ synthesis: Illustration on a freely available nonlinear aircraft benchmark, in Proceedings of the American Control Conference, pages 1303–1308, Chicago, IL, 2015.